Monitoring change in volcanic interiors using coda wave interferometry: Application to Arenal Volcano, Costa Rica

Roel Snieder

Center for Wave Phenomena and Department of Geophysics, Colorado School of Mines, Golden, Colorado, USA

Mike Hagerty

Institute of Geological and Nuclear Sciences, South Gracefield, Lower Hutt, New Zealand

[1] Multiply scattered waves are a new tool for monitoring changes in the earth's subsurface. In this study we use the air pressure and displacement recorded at the Arenal Volcano to detect temporal changes. The pressure pulses emitted by the volcano are associated with a complex displacement signal of overlapping coda waves. By deconvolving the ground motion with the air pressure for different time intervals we obtain a highly repeatable displacement signal that has the character of diffusive wave propagation. This deconvolved displacement signal changes with the time interval analyzed in the employed data. This change can be explained by a shift in the point of excitation of the elastic waves over a distance of about 15 meters.   INDEX TERMS: 7223 Seismology: Seismic hazard assessment and prediction; 7280 Seismology: Volcano seismology (8419); 7294 Seismology: Instruments and techniques. **Citation:** Snieder, R., and M. Hagerty (2004), Monitoring change in volcanic interiors using coda wave interferometry: Application to Arenal Volcano, Costa Rica, *Geophys. Res. Lett.*, *31*, L09608, doi:10.1029/2004GL019670.

1. Introduction

[2] The interior of volcanoes is highly heterogenous, leading to strong scattering of seismic waves. *Wegler and Lühr* [2001] showed that seismic waves generated by an airgun at Merapi are strongly scattered; the recorded coda waves have the signature of diffuse waves whose propagation is more like Brownian motion than ballistic propagation along rays. They inferred that the mean free path of the S-waves is only 100 m, much less than the size of the volcano.

[3] Multiply scattered waves are sensitive to small changes in a medium since their propagation path is long in a limited region of space. This property forms the basis of Coda Wave Interferometry [*Snieder et al.*, 2002; *Snieder*, 2002]. In this time-lapse technique, the change in multiply scattered waves for a given source-receiver pair is used to make inferences about the change in the medium or in the source position. The change in the coda waves is measured by computing the time-shifted cross-correlation before and after the change.

[4] Coda wave interferometry requires a repeatable source. In active source experiments, such as the study of *Wegler et al.* [1999], who used an airgun in a water basin, this condition is satisfied. When passive sources are used, one needs to establish independently to what extent the source changes with time. Earthquake multiplets have been used for time-lapse measurements of the Earth's structure [*Ratdomopurbo and Poupinet*, 1995; *Baisch and Bokelmann*, 2001; *Vidale and Li*, 2003; *Niu et al.*, 2003]. In this work we study the feasibility of using the air pressure and displacement [*Hagerty et al.*, 2000] recorded on Arenal Volcano, Costa Rica, in order to detect short-term temporal changes in the structure of the volcano or the excitation mechanism of these waves.

2. The Employed Data

[5] Arenal Volcano is a young (approximately 3,000 years old) stratovolcano located in northern Costa Rica. It was considered extinct prior to an explosive eruption in 1968, and, since 1984 it has primarily exhibited strombolian activity characterized by small but frequent summit explosions. A broadband seismic and geodetic network was installed around the flanks of Arenal in 1995, and in 1997 a five-element linear array of seismometers and microphones was temporarily deployed on the western flank to record the seismic-acoustic wavefield [*Hagerty et al.*, 2000]. In this paper we examine an approximately 16-min period of the seismic and acoustic signals recorded at a single site, approximately 2 km from the summit, during the 1997 deployment.

[6] The air pressure and ground motion were measured at the same location about 2 km from the summit with a Bruel and Kjaer low-frequency condensor microphone and an STS-2 seismometer, respectively [*Hagerty et al.*, 2000]. The pressure and displacement signals used in this study are shown in Figure 1. The pressure signal shows that the volcano goes through different dynamic regimes. For $t < -600$ s the pressure has a chaotic appearance; perhaps due to the short temporal spacing of the pressure pulses. The amplitude grows around $t = -600$ s, and for -600 s $< t <$ 150 s the pressure is dominated by a sequence of sharp pulses that have an amplitude and a pulse-interval that changes slowly with time. During the first half of this sequence, the pulse-interval increases. Around $t = -280$ s, the pulse-interval is suddenly halved. For the remaining part of the sequence, up to $t = 150$ s, the period again slowly increases. At that time the pulse-interval is again halved. The pattern is terminated by seismic events around $t = 175$ s. The presssure pulses at Arenal are postulated to be triggered in the shallow parts of the magma conduit by violent degassing caused by pressure drops [*Garcés et al.*, 1998].
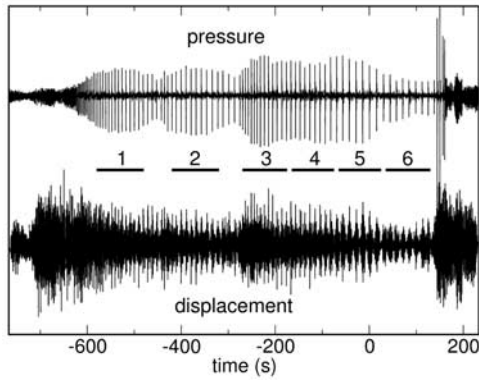
Figure 1. Air pressure and displacement recorded on Arenal. The pressure variations are about 20 Pa, while the maximum of the displacement corresponds to a particle velocity of about 1.5 μm/s. The numbers indicate the six intervals (ages) that are used for the deconvolution of the displacement data with the pressure data.

[7] The displacement, as shown in the bottom trace of Figure 1 does not have the impulsive character of the pressure. The later parts of the signal, around $t = 50$ s, shows that each pressure pulse is associated with an extended wave train in the displacement. This suggests that each pressure pulse generates a wave train in the displacement. When the pulse-interval is shorter, for example around $t = -550$ s, the individual wave trains in the displacement are longer than the pulse-interval, so that at that time the displacement has the appearance of random noise.

3. Extracting the Impulse Response From the Data

[8] In order to use the seismic data to detect temporal changes, it is necessary to extract the displacement impulse response from the data. We assume that each pressure pulse is associated with the excitation of elastic waves. If this is the case, then a deconvolution of the displacement $u(t)$ with the pressure $p(t)$ gives the response of the displacement that is associated with a single pressure pulse. In this study we carried out the deconvolution in the frequency domain with a water-level regularization, i.e., the deconvolved signal $D(\omega)$ in the frequency domain is given by

$$D(\omega) = \frac{u(\omega)p^*(\omega)}{|p(\omega)|^2 + \varepsilon}. \tag{1}$$

The regularization parameter ε was chosen to be 10% of the mean of the power of the pressure $|p(\omega)|^2$. Apart from this regularization no other damping or filtering was applied to the data.

[9] The deconvolution was applied to the six time intervals shown in Figure 1. We refer to the time of the different intervals as *age*, and use the word *time* exclusively for the time within each interval. The intervals each have a length of 100 s, and are chosen to be centered on different regimes of the pressure pulses. Since these intervals do not overlap, each interval provides an independent estimate of the

impulse response of the displacement. The six deconvolved waveforms are shown in Figure 2.

[10] For $t < -5$ s these deconvolved waveforms consist of uncorrelated random noise with a noise level that is significant compared to the coherent part of the wave field around $t = 0$ s. This is not surprising; the pressure signal in the top trace of Figure 1 has a significant noise contamination between the pressure pulses. That noise contamination may be aggravated by any noise that is hidden on the displacement signal in the bottom trace of Figure 1.

[11] For times between -4 s and around 6 s the deconvolved waveforms are highly correlated. The only exception is the deconvolved signal for age 6, perhaps because of the lower signal level at that age. Because the deconvolved waves computed for the different ages are coherent after about -4 s, we judge that the impulse response in the deconvolved waves starts around that time. This does not mean, however, that the response of Arenal is acausal. The time difference between the arrival time of the pressure signal and the displacement is about 5 s. This agrees with the observed emergence of the signal in the deconvolved waveforms around $t = -4$ s.

[12] The deconvolved waveforms have the character of diffusive waves; the coda slowly builds to a maximum at around $t = 0$ s, and then decays again. Superposed on these coda waves are distinct arrivals around $t = -3$ s and $t = 0$ s. The wave at $t = 0$ s may be due to the coupling of the air wave either to the ground motion or directly to the seismometer. Since the microphone and the seismometer are at the same location this wave arrives at $t = 0$ s. The waves arriving between -4 s and 6 s have a general character similar to the diffusive waves that have been reported for other volcanoes [*Wegler and Lühr*, 2001; *Ratdomopurbo and Poupinet*, 1995]. The dashed line in the bottom trace of Figure 2 shows the amplitude obtained by taking the square root of the solution of the 3D diffusion equation:

$$I = \frac{A}{(t - t_0)^{3/2}} \exp\left(-\frac{r^2}{4d(t - t_0)} - b(t - t_0)\right) + n \tag{2}$$

In this solution we used the following parameter values: $A = 6.25 \times 10^4$, $t_0 = -5$ s, $d = 0.03$ km^2/s, $r = 2$ km, $b = 0.8$ s^{-1},
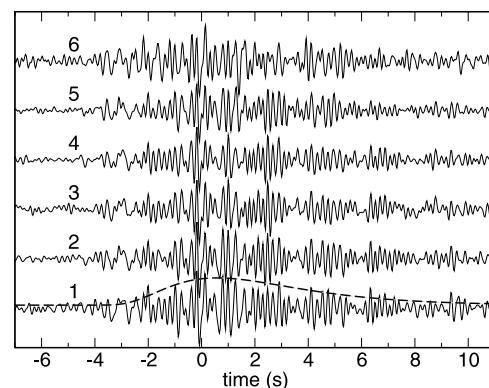

Figure 2. Deconvolved displacement for the six ages shown in Figure 1. The numbers near each trace indicate the employed age. The dashed line gives the amplitude computed from the diffusive solution (2).
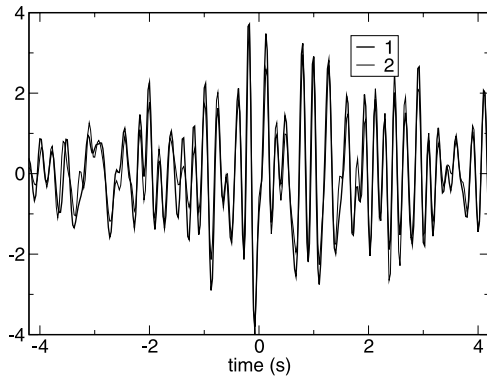
Figure 3. Enlargement of the deconvolved waveforms computed for ages 1 and 2.

and $n = 0.09$. The parameters b and d, that characterize the attenuation and scattering, respectively, are close to the values obtained by *Wegler and Lühr* [2001] for Merapi.

[13] The deconvolved waveforms are most similar for adjacent ages. The early part of the deconvolved waveforms for the ages 1 and 2, shown in Figure 3, exhibit large similarity of these waveforms. As can be seen in Figure 2, this similarity decreases when the deconvolved wave from age 1 is compared with the deconvolved waves from progressively later ages.

4. The Correlation of the Deconvolved Signals

[14] In this section we outline the theory of coda wave interferometry [*Snieder et al.*, 2002; *Snieder*, 2002]. In this technique the time-shifted correlation coefficient of two signals $u_1(t)$ and $u_2(t)$ is used to quantify the degree of similarity of the signals. This coefficient is defined as

$$R(\tau) = \frac{\int_{t-T}^{t+T} u_1(t')u_2(t' + \tau)dt'}{\sqrt{\int_{t-T}^{t+T} u_1^2(t')dt' \int_{t-T}^{t+T} u_2^2(t')dt'}}. \tag{3}$$

The integration is over a time interval with duration $2T$ and center time t. By computing this correlation coefficient for windows with a different center time t one can infer the velocity change of the medium between the recording of the waveforms $u_1(t)$ and $u_2(t)$. Coda wave interferometry is based on path summation, wherein the signal is decomposed into a sum over all scattering paths, and all possible mode conversions [*Snieder*, 1999, 2002]. When the medium changes, the travel time of the wave along each path changes. The cross-correlation reaches its maximum at a time that is given by the mean travel time change over all paths. This mean is weighted by the energy of each arrival in the path summation. In the absence of noise, the value $R_{\max}$ of the correlation coefficient at its maximum is related to the variance of the travel time perturbation, σ_t^2, by

$$R_{\max} = 1 - \frac{1}{2}\overline{\omega^2}\sigma_t^2, \tag{4}$$

where the variance is computed with the energy of each arrival as weight for each arrival. The frequency $\overline{\omega^2}$ is given by

$$\overline{\omega^2} = \frac{\int_{t-T}^{t+T} \dot{u}^2(t')dt'}{\int_{t-T}^{t+T} u^2(t')dt'}. \tag{5}$$

[15] We computed the time-shifted cross-correlation between the deconvolved waves in Figure 1 for different pairs of ages. The location of the maximum of the time-shifted cross-correlation does not depart significantly from the unshifted position $\tau = 0$. This is the case for both the early part $(-4 < t < 0$ s$)$ as well as for the later part $(0 < t < 4$ s$)$ of the coda. This means that the velocity of wave propagation did not change with age.

[16] Visual inspection of Figure 2 shows that the deconvolved waveforms themselves do change with age. The zero-lag cross-correlation computed for the time interval $-2.5 < t < 7.5$ s of the deconvolved wave from age 1 with the deconvolved waves from the other ages is shown in Table 1. The cross-correlation generally decreases with increasing age; indicative that the deconvolved waves change with age. The noise level in the deconvolved waves reduces the cross-correlation and causes a bias in the estimate of the correlation coefficient. The cross-correlation can be corrected for this bias. The cross-correlation R_{corr} that is corrected for the bias due to random noise is related to the cross-correlation from expression (3) by

$$R_{corr} = R \Big/ \sqrt{1 - \frac{\langle n_1^2 \rangle}{\langle u_1^2 \rangle}} \sqrt{1 - \frac{\langle n_2^2 \rangle}{\langle u_2^2 \rangle}}, \tag{6}$$

where $\langle u_{1,2}^2 \rangle$ is the mean value of the energy of the noise-corrupted data, and $\langle n_{1,2}^2 \rangle$ is the mean energy of the noise. The noise energy is estimated from the deconvolved waves over the time range -20 s $< t < -10$ s. The corrected cross-correlation is shown in the third column of Table 1. Note that the increase in the cross-correlation after the noise correction is fairly small.

5. A Model to Explain the Change of the Waves

[17] Since the deconvolved waves do not display a time-shift with age, it is unlikely that these waves decorrelate because of a change in the seismic velocity in Arenal. Given the short duration of the employed data, about 16 min, this is not surprising. It is more likely that during this interval

Table 1. The Correlation Coefficient R, the Noise-Corrected Correlation Coefficient R_{corr}, the Standard Deviation σ_t of the Travel Time Perturbation, and the Associated Change in the Source Location δ, Computed by Comparing the Deconvolved Waves From Time Age 1 With Those From the Later Ages

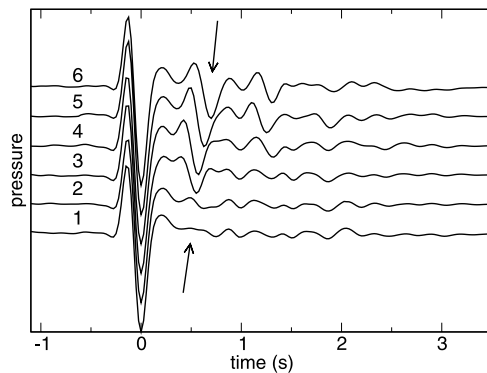| ages	R	R_{corr}	σ_t (s)	δ (m)
1–2	0.949	0.996	0.0032	3.1
1–3	0.857	0.911	0.0151	16.3
1–4	0.886	0.927	0.0137	14.8
1–5	0.886	0.930	0.0134	14.8
1–6	0.746	0.802	0.0226	24.5

Figure 4. The average pressure pulses for each of the six ages of Figure 1. The individual pressure pulses were normalized before averaging.

the source of the seismic waves changes. The source can change in either of two ways: the source signal may change or the source location can change. We averaged the pressure pulses shown in the top trace of Figure 1 over the six ages (Figure 4). Each pressure pulse was normalized to a uniform amplitude before averaging. The main pressure pulse for the six intervals is highly repeatable. The waves that arrive after the main pulse, however, change in a systemic way from one age to the next. Nevertheless, since the main pulse around $t = 0$ carries most energy, we conclude that for all practical purposes the source signal is unchanged.

[18] In the following we assume that the deconvolved waves in Figure 2 change because of a temporal change in the source location. Although we cannot give a proof that this is the cause of the change in the deconvolved waves, we can estimate the change in the source location required to give the measured cross-correlation. This estimate is based on the theory for coda wave interferometry for changes in the source location [*Snieder*, 2003], and is based on the following ideas. When the source is displaced, the distance of the source to some scatterers increases, while the distance from the source to other scatterers decreases. This changes the arrival times of the waves that interfere to give the coda. The resulting decorrelation of the waves for the original source and the displaced source is related to the variance of the travel-time perturbation for the different waves by expression (4).

[19] The relation between the cross-correlation and the change in the source location depends on the source mechanism, but it is not clear what is the source mechanism of these waves. Here we assume that the pressure pulses act like an isotropic point source for the seismic waves. In that case the change in the source location δ is related to the standard deviation σ_t of the travel time perturbation by [*Snieder*, 2003]

$$\delta = \sqrt{3} v_P \sigma_t, \qquad (7)$$

where v_P is the P-velocity, and where σ_t is estimated from the cross-correlation of the deconvolved waves by expression (4). In that expression $\overline{\omega^2}$ is obtained from the data using expression (5). From these data $\overline{\omega^2}$ corresponds to an average frequency of about 5 Hz. The standard deviation σ_t of the travel-time perturbation, computed from the corrected

correlation coefficient R_{corr}, is shown in the fourth column of Table 1. For the correlation of age 1 with that of ages 3 through 5, this standard deviation is about 0.015 s. For a frequency of 5 Hz this corresponds to about 1/12th of a period.

[20] Assuming a P-wave velocity of 2500 m/s [*Murase and McBirney*, 1973; *Hagerty et al.*, 2000], this time change corresponds to the change in the source location shown in the last column of Table 1. The change in the source location, which is of the order of 15 m between age 1 and the later ages, should be taken with a grain of salt. The model of an isotropic source is fairly arbitrary, and the value of the P-velocity is not based on any measurement. A change in the location of the source of the pressure pulses over a distance of about 15 m over 1000 s is not unrealistically large when compared to the size of the conduits and magma chambers in a volcano. This means that the decorrelation of the deconvolved waveforms can readily be explained by a change in the source location.

[21] The averaged pressure pulses in Figure 4 show a secondary phase (indicated by arrows) that moves to later times with age. It is not clear how this secondary phase is generated. It may be generated by a reflected wave or by a resonance in the fluids or gasses that generate the pressure pulses. A change in the position of the source of the pressure pulses could change the excitation of the resonating modes, which could result in a change of the secondary phase in the source signal.

6. Conclusions

[22] The deconvolution of the displacement with the pressure for the employed six ages leads to highly reproducible deconvolved waveforms. The deconvolution used here is a simple process that can be carried out automatically in real-time. When applied to longer time intervals, this may open the possibility to conduct volcano monitoring based on coda wave interferometry without using an active source.

[23] The deconvolved waveforms slowly change with age. Assuming that this change is caused by a change in the source position, and assuming that the source is an isotropic point source, the changed waveforms can be explained by a displacement in the source position of about 15 m. Although his number is not particularly accurate, its order of magnitude is small compared to the size of the interior structure of the volcano. If the employed interpretation is correct, then coda wave interferometry can be used to infer small changes in the location of the pressure pulses that are generated at active volcanoes.

References

Baisch, S., and G. Bokelmann (2001), Seismic waveform attributes before and after the Loma Prieta earthquake: Scattering change near the earthquake and temporal recovery, *J. Geophys. Res.*, *106*(B8), 16,323–16,337.

Garcés, M., M. Hagerty, and S. Schwartz (1998), Magma acoustics and time-varying melt properties at Arenal Volcano, Costa Rica, *Geophys. Res. Lett.*, *25*(13), 2293–2296.

Hagerty, M., S. Schwartz, M. Garcés, and M. Protti (2000), Analysis of seismic and acoustic observations at Arenal Volcano, Costa Rica, 1995–1997, *J. Volcanol. Geotherm. Res.*, *101*, 27–65.

Murase, T., and A. McBirney (1973), Properties of common igneous rocks and their melts at high temperatures, *Geol. Soc. Am. Bull.*, *84*, 3563–3592.

Niu, F., P. Silver, R. Nadeau, and T. McEvilly (2003), Migration of seismic scatterers associated with the 1993 Parkfield aseismic transient event, *Nature*, *426*, 544–548.

Ratdomopurbo, A., and G. Poupinet (1995), Monitoring a temporal change of seismic velocity in a volcano: Application to the 1992 eruption of Mt. Merapi (Indonesia), *Geophys. Res. Lett.*, *22*(7), 775–778.

Snieder, R. (1999), Imaging and averaging in complex media, in *Diffuse waves in complex media*, edited by J. Fouque, pp. 405–454, Kluwer, Dordrecht.

Snieder, R. (2002), Coda wave interferometry and the equilibration of energy in elastic media, *Phys. Rev. E*, *66*, 046615, doi:10.1103/PhysRevE. 66.046615.

Snieder, R. (2003), Constraining relative source locations with the seismic coda, in *Project Review of the Consortium Project on Seismic Inverse Methods for Complex Structures*, pp. 207–216, Center for Wave Phenomena, Colorado School of Mines, Golden, Colorado.

Snieder, R., A. Grêt, H. Douma, and J. Scales (2002), Coda wave interferometry for estimating nonlinear behavior in seismic velocity, *Science*, *295*, 2253–2255.

Vidale, J., and Y. Li (2003), Damage to the shallow Landers fault from the nearby Hector Mine earthquake, *Nature*, *421*, 524–526.

Wegler, U., and B. Lühr (2001), Scattering behaviour at Merapi volcano (Java) revealed from an active seismic experiment, *Geophys. J. Int.*, *145*, 579–592.

Wegler, U., B. Lühr, and A. Ratdomopurbo (1999), A repeatable seismic source for tomography at volcanoes, *Ann. di Geofisica*, *42*, 565–571.

————————————

R. Snieder, Department of Geophysics, Colorado School of Mines, Golden, CO 80401-1887, USA. (rsnieder@mines.edu)

M. Hagerty, Institute of Geological and Nuclear Sciences, 41 Bell Rd., South Gracefield, Lower Hutt, New Zealand. (m.hagerty@gns.cri.nz)